Quantum, Solid-state, Plasma and Vacuum Electronics

https://doi.org/10.32603/1993-8985-2019-22-5-93-106

Original article

From Gas Sensors to Detection of Etanol Vapour to Sensor of Bacteria Detection

Dimitre Tz. Dimitrov✉

Sofia University St. Kliment Ohridski, Sofia, Bulgaria

✉ nhddt@chem.uni-sofia.bg, dimitrov2001@yahoo.com

Abstract

Introduction. Metal oxide semiconductor sensors have many advantages. But their working temperature is still high and their sensitivities are frequently low. In the current work, I present the results from investigation of sensing ability of new kind of potentiometric solid state gas sensor.

Aim. The main goal of this work is investigation of the temperature dependence in the flow of air and in ethanol vapour mixture of the investigated junction structures. Also, we investigated at fixed temperature the dependence of the thermoelectric force from the ethanol vapour concentration at possible low operation temperature. For the structure, which shows the lowest operation temperature to ethanol vapour, we investigate the ability to detect *Pseudomonas putida* suspension.

Materials and methods. In this work, the sensitivity to ethanol vapour and *Pseudomonas putida* suspension were investigated by measuring the thermoelectric force (the voltage) appearing of the structures by standart voltmeters.

Results. Two experimental installations for sensors have been developed. The first one is for detection of ethanol vapour by ZnO/ZnO:Cu, ZnO/ZnO:CuO, ZnO/ZnO:Fe junction structures. The second installation was for *Pseudomonas putida* suspension detection in gas phase by ZnO/ZnO:Fe junction structure. We discovered that ZnO/ZnO:Fe structure, has the lowest operation temperature of 200 °C to ethanol vapour. For this structure, the potential difference has a negative value and decreases with increasing the amount of the pulverized bacteria.

Conclusion. We discovered that ZnO/ZnO:Fe structure, has the lowest operation temperature of 200 °C. This operation temperature is a bit higher than operation temperature of at which some very novel sensing structures shows the maximum sensitivity.

Key words: Nanostructured ZnO thin films, Ga and Cu doped ZnO thin films, CuO doped ZnO nanowires, Fe doped ZnO thin films, Ethanol gas sensor and Bacteria detection

Conflict of interest. I declare that this work has no conflict of interest.

Introduction. The basic principle of operation of the solid state ethanol sensors are the changes of the electricalproperties of ZnO layer under adsorption of ethanol molecules on the ZnO surface. The interaction of ethanol molecules with ZnO surface is investigated and understood quite well [1, 2]. Taking into account very poor selectivity of ZnO gas sensors, the molecules of ethanol gas could be used as a probe for checking sensing properties of the ZnO gas sensors.

Different science groups have fabricated solid-state ethanol sensors in the form of sensing film, formed on alumina ceramic tube, different nanostructures on flat solid surfaces, different forms of chemoresistors, formed by pressing, powder of ZnO nanoparticles used for generated cataluminescence emission from catalytic ethanol oxidation on the surface.

The normal operation temperature of metal oxide gas sensors is in general within the range between 200 and 500 °C, where conduction is electronic and oxygen vacancies are doubly ionized. ZnO thin films, one of the earliest discovered material for gas sensing has been widely used to detect low-concentration of gases, have drawbacks, for instance, the working temperature is within the above range and their sensitivities are frequently low [3].

Real-time detection of toxic gases by analytical

93

equipments such as Fourier transform infrared spectroscopy, Gas chromatography, or mass spectrometers is expensive and not practical mainly due to the bulky size of the instruments. Metal oxide semiconductor sensors have advantages of small size, low mass and cost, good sensitivity at the ambient conditions, easy processing and simplicity in fabrication [4, 5].

In the current work, I present the results from investigation of sensing ability of new kind of potentiometric solid state gas sensors, which are having nonlinear response towards the ethanol vapour concentration. In this work:

1. The sensing structures were constructed by overlapping of pure ZnO and doped with Cu or Ga nanostructured ZnO layers and their sensing properties investigated in the temperature range from 240 to 350 °C. By using thus constructed by us apparatus, presented in detail here, we investigated first the temperature dependence in the flow of air and in ethanol vapour mixture. Second, we investigated at fixed temperature the dependence of the thermoelectric force (the potential difference) appearing on the junctions from the ethanol vapour concentration [6].

2. Described the synthesis of ZnO/ZnO:CuO structures in the form of overlapping layers of nanowires of pure and copper oxide doped zinc oxide. The obtained structures were tested as a sensor to the vapour of ethanol. Interaction of the obtained sensor structures with vapour of ethanol is investigated by measuring the potential difference between the layers of pure and CuO modified ZnO nanowires in the temperature range from 190 to 300 °C [7].

3. Ivestigate the nostructured layers ZnO/ZnO:Fe junctions, obtained by the sol-gel technology. The best sensing performance was obtained for the structure with upper layer produced by two dip-coatings in the sol containing 3 at. % of Fe into it in the temperature range from 180 to 360 °C [8].

Taking into account that ZnO/ZnO:Fe junction structures has significant sensitivity to ethanol vapour at lowest operation temperature and that during sensing of ethanol, there is a chemical interaction between oxygen of ethanol and zinc of ZnO:Fe thin film [9] and the fact that leaching of Zn ions has a minor influence on the antibacterial activity [10], we concluded that ZnO/ZnO:Fe junction structures can be used for detection of bacteria. We use an experimental investigation of the sensing properties towards *Pseudomonas putida* suspension of the ZnO/ZnO:Fe junctions. The sensing properties of these structures towards *Pseudomonas putida* suspension are investigated in a newly constructed experimental set-up for bacterial detection [11, 12]. Observed properties depend on the relation of the concentration of charge carriers into the top and the bottom layers of the sensing junction and the nature of analyte.

Materials and methods. The main purpose of this work is to check the sensing to traces of ethanol vapour of different junction structures (ZnO/ZnO:Cu,Ga, ZnO/ZnO:CuO, ZnO/ZnO:Fe). After that the ZnO/ZnO:Fe structures, which shows the best sensitivity at ethanol vapour at lowest operation temperature were tested in detection *Pseudomonas putida* suspension.

1. *Preparation of* ZnO/ZnO:Cu,Ga *structures* [6]. For preparation of ZnO doped with Cu and Ga sol we have used the following precursors: $Zn(CH_3COO)_2 \cdot 2H_2O$ and 2-methoxyethanol, both from Fluka, monoethanolamine from Riedel-de-Haen, $Cu_2(OAc)_4 \cdot 2H_2O$ from Sigma and Ga(III) chloride from Aldrich. Three different sols with concentration of Cu and Ga as 1, 3 and 5 at. % into it were prepared. The nanostructured layers were deposited on alumina ceramic substrate (Rubalit®710) with size 20×10×0.63 mm from CeramTec AG. The precursors were mixed together in a round bottom triple neck flask, stirred by magnetic stirrer for 15 min at room temperature and heated to 60 °C while stirring for 1 h. The produced by the above way sol was aged for 24 h. The process of producing the structures including pure and doped with Cu and Ga ZnO films consist of two stages, each including of few steps. The first stage is preparation of thin film of ZnO if we want the ZnO layer to be lower layer of the structure and the second is preparing the doped layer by earlier prepared solutions with different content of Cu and Ga, when we want the doped layer to be on the top of the structure. The process of producing pure ZnO thin films consists of the following steps:

a) deposition of the sol on ceramic substrate Rubalit®710 by means of dip-coating method;

b) different numbers of dip-coating cycles of the substrate into the sol until obtaining the desirable thickness of the films;

c) drying and annealing of the films.

After each dipping procedure the films were drying at 80 °C for 30 min and then dipped again into the sol until the desirable thickness was obtained. The final calcination of a film is carried out at 500 °C for 60 min, followed by cooling down in the air at the room temperature. ZnO films doped with Cu or Ga were prepared by the same procedure, us-

From Gas Sensors to Detection of Etanol Vapour to Sensor of Bacteria Detection

ing different amounts (1, 3 or 5 at. %) of the dopants: $Cu_2(OAc)_4 \cdot 4H_2O$ (Sigma), or $Ga(III)Cl_3$ (Aldrich). Different samples with different numbers of dip-coating cycles in the sol and different constructions were produced. The structures ZnO/ZnO:Cu or Ga, in which pure ZnO as a bottom layer was overlapped by the upper part with doped ZnO, and vise versa. The area of the overlap between the lower and upper layers were kept ~ 80 mm^2.

2. *Preparation of* ZnO/ZnO:CuO *nanowires structures* [7]. The synthesis of ZnO nanowires on a solid substrate consisted of two stages, namely, the deposition of a layer of nuclei and nanowire growth. A layer of nuclei was applied from a $Zn(CH_3COO)_2$ solution with a concentration of 5 mmol/L by centrifuging (KW-4A (Chemat Technology Inc.) centrifuge) at a speed of 900 rpm for 10 s and at a speed of 2200 rpm for 20 s followed by air drying. This operation was repeated five times to prepare a layer of ZnO nuclei that can be used for nanowire growth. The substrate was then washed, dried, and annealed at 320 °C for 20 min. The entire process of creating nuclei on a substrate was repeated two times, and the substrate with an applied layer of nuclei was washed with distilled water and dried in air. Nanowires were then grown on these substrates from precursor solutions. Solutions $Zn(NO_3)_2 \ 6H_2O$ (Sigma_Aldrich, purum p.a. ≥ 99.0 %) and metheneamine (Merck, purum p.a. ≥ 99.5 %) with a concentration of 50 mmol/L were mixed in the same volumes immediately before the beginning of each growth cycle. The final concentration of each reagent in the precursor solution was 25 mmol/L. Samples were vertically placed in the solution and held at 87 °C for 3 h. The substrates were then removed from the solution, washed with distilled water, and located in an as-prepared precursor solution. The growth process was repeated eight times. The prepared layers of zinc oxide nanowires were washed with acetone and distilled water and then dried in air.

For our investigation, it was necessary to form a layer of pure ZnO nanowires that is overlapped with a layer of CuO-doped ZnO nanowires. Such samples were prepared by the immersion of a layer of nanowires to two-thirds of their length into a $Cu(NO_3)_2 \cdot 3H_2O$ solution (Valerus, purum p.a. ≥ 99.0 %) with a concentration of 10 mmol/L. The samples were dried at 75 °C for 10 min in air, and the process of immersion was repeated two, four, or six times to grow modified layers with various CuO concentrations. The samples were annealed at 300 °C for 10 min.

3. *Preparation of* ZnO/ZnO:Fe *structures* [8, 12]. Zinc acetate dehydrate $\left[Zn(CH_3COO)_2 \cdot H_2O \right]$, 2-methoxyethanol, mono-ethanolamine (MEA) and iron nitrate hydrate, $\left[Fe(NO_3)_3 \cdot 9H_2O \right]$ were purchased from Fluka. Ceramic substrates Rubalit®710 (20×10×0.63 mm and 25×15×0.63 mm) were purchased from CeramTec AG and were used as supports for the films. Nanostructured ZnO:Fe thin films were formed on a ceramic substrate via dip-coating technique from sol. The sol was prepared by dissolving $Zn(CH_3COO)_2 \cdot 2H_2O$ and $Fe(NO_3)_3 \cdot 9H_2O$ in 2-methoxyethanol, to which a weak base MEA was subsequently added. The junctions, composed by two plane-parallel nanostructured thin film electrodes, were prepared as described below. The 2/3 of the entire area of the substrate Rubalit®710 was coveredfirstly by layer of pure ZnO, produced by three dip-coatings. Then, the same area on the opposite end of the sample was covered by ZnO layer doped with Fe. The overlapping area between the lowerand upper layers is kept ~ 80 mm^2 for all samples for etanol detection and ~ 125 mm^2 for bacteria detection. The sample swere produced with different thickness of the top layer by varyingthe number of dip-coatings. The films were dried at 80 °C for 30 min after each successive coating. Finally, when the desired thickness ofthe layer was reached, the sensing junction structure was annealed at 500 °C for 60 min.

Response of the investigated structure to ethanol vapour. *Test equipment.* In the current work different sensing junction structures were tested by means of novel in-house made experimental setup specially designed for investigating the temperature dependence of the potential difference of the different junction structures in the continuous air flow and the changes in the value of the potential difference when these structures are exposed to mixture of vapour of ethanol with air flow. The scheme of this equipment is shown on Fig. 1 [6] (*1, 2* – gas cylinders with technical air; *3, 4* – security air locks; *5* – flowmeter for measuring the tiny gas flows (ethanol vapour flow); *6* – flowmeter for measuring the air flow; *7, 8* – drexels with silicagel; *9* – drexel with ethanol; *10* – threefold gas mixer; *11* – aluminium head of the quartz tube; *12* – voltmeter for measuring the potential difference between the overlapped layers; *13* – metal stick, carrying the ceramic sample holder; *14* – quartz tube; *15* – ceramic holder with the sample; *16, 17* – metal pressing-point electrodes, making Ohmic contacts with the sample; *18* – tube heater; *19* – outlet drexel with glycerin [6]).
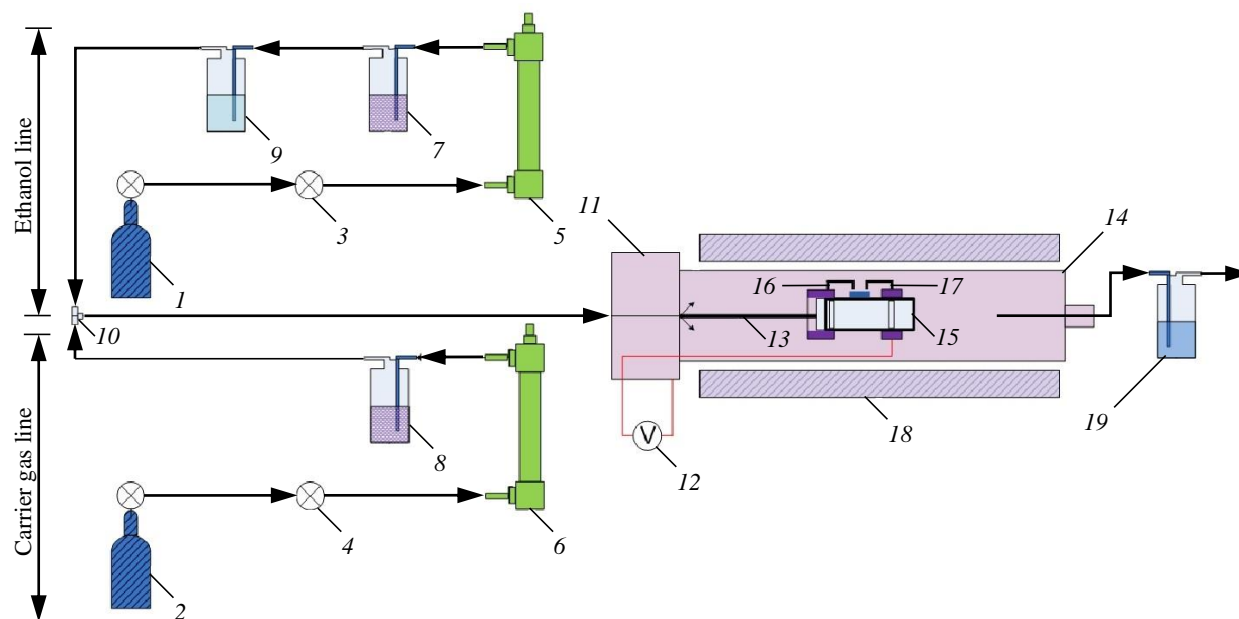
Fig. 1. Scheme of experimental setup

As it can be seen from Fig. 1, by the use of the above measuring equipment we were able to measure the thermoelectric potential difference, ΔU, appearing between the overlapped two parts of the investigated structures. The electric circuit is formed between two overlapped at 80 mm^2 pure and doped with Cu or Ga ZnO layers (ZnO/ZnO:Cu,Ga), pure and doped with CuO layers of nanowires ZnO (ZnO/ZnO:CuO), pure and doped with Fe layers of ZnO (ZnO/ZnO:Fe). At the end of the upper and lower layers of the sensing junction, at about 1…2 mm from the point of the overlap, two point needled electrodes *16*, *17*, made from stainless steel are pressing on the layers, making Ohmic contacts of the metal to the semiconductor. The needle electrode, connected to the lower layer is attached to the metal stick, carrying the ceramic sample holder. The ceramic holder is connected to the aluminum head of the quartz tube, from where a connector is going to the common input of the voltmeter *12*.

The other needle electrode, connected to the upper layer is connected through isolated thermo resistive wire to the other input of the same Voltmeter. By this way, voltmeter *12* is connected to the both wires, coming from the sample and measures the potential difference between the overlapped two layers of the sensing structure.

The ceramic holder *15*, together with sample attached by pressing with two metal electrodes is placed onto the quartz tube *14*. The tube heater *18* is used for heating quartz tube together with the sam-

ple. The tube heater is supplied by its own power supply, which allows slowly changing of the temperature. After the desired value of the temperature was reached, it was kept stable by means of Voltage Stabilized (not shown on Fig. 1). The temperature was measured by standard thermocouple Chromel-Alumel, connected to other Voltmeter. Mixing of the flows of the ethanol vapour with dry air provides the particular ethanol concentration. The flowing of air for ethanol and dry gas lines are provided by standard bottles of dry air under high pressure *1*, *2*, with standard reducing valves on each. From the bottles of air, flows goes through security air locks. Air locks are connected to the flowmeters *5*, *6*, which needles' valves allows regulation of the air flows very precisely. After this, the flows goes through two Drexels with silicagel *7*, *8* for filtration and additional drying of the air. After that, the tiny gas flow goes into the Drexel with ethanol *9*, where the air is saturated with ethanol vapour. These two flows, the dry air and the saturated with ethanol vapour air flow, were mixed by three-fold gas mixer *10*. After mixing, the resulting flow with certain known concentration of ethanol vapour goes into the quartz tube and gets into contact with the sample. For preventing an outside flow into the experimental system, at the output the gas mixture goes through Drexel with glycerin.

Results and discussions. 1. *Temperature dependence of the potential difference of obtained* ZnO/ZnO:Cu *junctions in air flow and in the flow of mixture of air with ethanol vapour with concentra-*

tion of 1500 ppm. For each of the samples the temperature dependence of the potential difference in air flow and in 1500 ppm concentration of ethanol vapour was investigated. The 1500 ppm concentration was produced by the mixing of flow of air and flow of saturated ethanol vapour.

Temperature dependence of the potential difference in the air and in the flow of mixture of ethanol vapou with air having concentration 1500 ppm for different ZnO/ZnO:Cu structures, upper layers of which is produced by certain number of dip-coating cycles into the having 3 at. % Cu sol is shown on Fig. 2 [6].

How it can be seen from Fig. 2, *a*, *b*, the behavior of the potential difference in the air flow with increasing the temperature is completely different for the samples with the top layer produced by two and three coating cycles into the Cu contained sol. In the case of upper layer produced by two dip-coating cycles the potential difference firstly increases with the temperature up to the value of about 2.35 mV at 290 °C and then decrease down to the value of about 1.5 mV at 303 °C (Fig. 2, *a*).

With increasing the temperature two processes are happening into the upper ZnO layer, which are account for observed on Fig. 2, *a* results:

1) because ZnO is an *n*-type semiconductor material, its resistance will decrease with increasing temperature because more electron-hole pairs are generated. Because of the electron-hole pairs generation, the thermoelectric coefficient α_{top} of the upper layer of the investigated structure is getting more negative value. That leads to the increase of the total potential difference as positive value;

2) oxygen ionosorption removes the conduction electrons from conduction band of ZnO and by this way increases its resistance. At temperatures fewer than 150 °C, the molecular species dominate, while

above this temperature the atomic species dominate, which can allow capturing one or two electrons from conduction band of ZnO with increasing of the temperature [13].

If we neglect the dependence of the Seebeck coefficient α on the temperature, the resulting expression for the potential difference ΔU takes the form [14]:

$$\Delta U = \Delta U_1 - \Delta U_2 = \left(\alpha_{bot} - \alpha_{top} \right) \Delta t.$$

Because of this process the thermoelectric coefficient α_{top} of upper layer is getting less negative value, which will make the total potential difference to decrease as positive value as can be considered from the formula. The observed on Fig. 2, *a* trend of the changing the total potential difference in the case of ZnO/ZnO:Cu structure, with upper layer produced by two dip-coatings cycles into the sol, containing 3 at. % Cu is a result of these two processes. The α_{top} of upper layer is increased as a negative value, up the temperature of 290 °C, because up to that temperature the generation of charge carriers in this layer more strongly affects the total potential difference of the sensing structure than the depletion layer, caused by the oxygen ionosorption on the surface of the overlap. As it can be seen, due to the dependence of the potential difference from the temperature in the atmosphere, the total potential difference is increasing up to 290 °C and is decreasing after that (Fig. 2, *a*).

The potential difference in the air flow has zero value up to 277 °C when the top layer is produced by three dip-coatings into the sol, after which gradually decreases as negative value down to −1.85 mV at the temperature 345 °C (Fig. 2, *b*). The reason for this could be understood by taking again into account formula. It could be seen that because of both α_{bot}
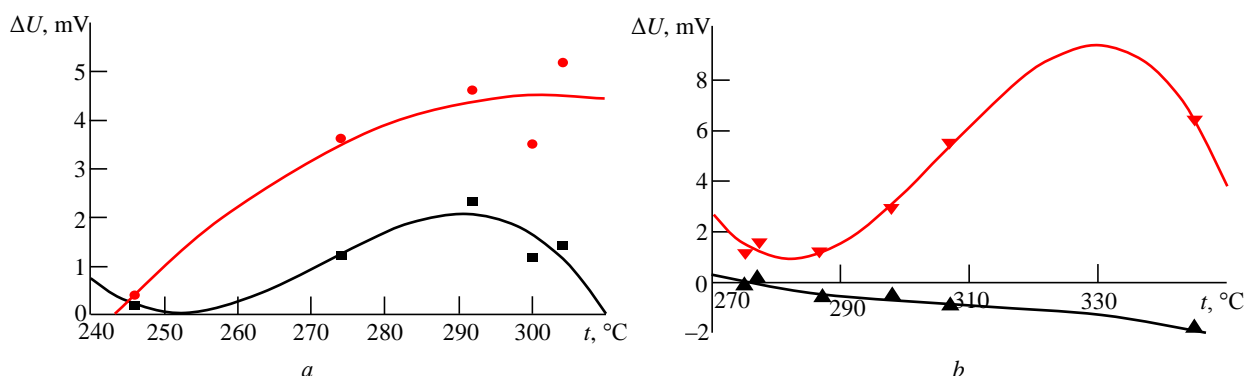

Fig. 2. Temperature dependence of the potential difference for ZnO/ZnO:Cu structures, with upper layer produced from the zol containing 3 at. % Cu by: *a* – two dip-coating cycles; where: ■ – at the air, ● − at ethanol vapour with concentration 1500 ppm; *b* – by three dip-coating cycles where ▲ − at the air, ▼ – at ethanol vapour with concentration 1500 ppm [6].

and α_{top} being negative, with the temperature increasing, the potential difference will be getting more negative value. This is possible when the thermoelectric coefficient α_{bot} of down layer has larger negative value than the thermoelectric coefficient α_{top} of upper layer, and the latest having not such a big negative value. The observed gradual increase of the potential difference as negative value could be happening when increasing the temperature leads to the electron-hole pair generation in the lower layer and has more pronounced effect than generation of electron-hole pairs in the upper layer. The thermoelectric coefficient α_{top} of upper layer won't have so negative value, and we will have small value of negative total potential difference, which will get more negative along with increasing the temperature, because it is determined mainly by the thermoelectric coefficient α_{bot} of the down layer. This probably is related to the increase degree of crystallization with increasing the size of the particles of the top film with increasing the number of coatings (Fig. 2, *b*), which was proven in one of our previous work [15]. The increased degree of crystallization will reduce the number of point defects, which are the main source of electrons into ZnO and by this will make the above mentioned effect of Cu doping more pronounced in the reduction of the number of electrons generated into the top layer.

2. *Ethanol vapour concentration dependence of* ZnO/ZnO:Cu *junction structures.* At the temperature at which each of the samples has the maximum value of the sensitivity, the dependence of the potential difference on the concentration of ethanol vapour was investigated. The dependence of the potential difference on the ethanol concentration for the samples with the different number of dip-coating cycles,

at the temperature where the sensitivity of the samples has the maximum value, is shown on Fig. 3 [7].

Measuring the ethanol concentration dependence of the samples at $t = 306 \pm 2$ °C and at $t = 300 \pm 2$ °C is done for the samples with upper layer produced by two and three dip-coating cycles, respectively.

Results for both of the samples show that no matter of the numbers of dip-coating cycles, with each upper layer is produced, the potential difference increases nonlinearly as a function of ethanol concentration. The concentration of electrons n_{bot} in the layer on the bottom of the sensing structure doesn't change during the ethanol detection at constant temperature. However, during the interaction with ethanol, due to the transfer of electrons between the adsorbed on the ZnO surface oxygen ions, attracted are one or two electrons from the conduction band of ZnO. The concentration of electrons n_{top} in the top layer of sensing structure (doped with Cu ZnO) will change. Those oxygen ions interact with ethanol molecules, and return back captured one or two electron into the conduction band of ZnO, and that leads to increasing of the concentration of electrons n_{top} in the top layer of sensing structure. This will give the nonlinear trend of the change of the total potential difference ΔU with the change of the concentration of ethanol vapour. It can be seen that with increasing the concentration of ethanol, the potential difference is increasing nonlinearly and for the sample, having upper layer produced by 3 dip-coating cycles, increasing is much more. In both of the cases increasing comes to saturation and for two dip coating cycles sample, saturation comes early, even thought the sensitivity is less.

3. *Temperature dependence of the potential difference of obtained* ZnO/ZnO:CuO *nanowires junctions in air flow and in the flow of mixture of air with etha-*
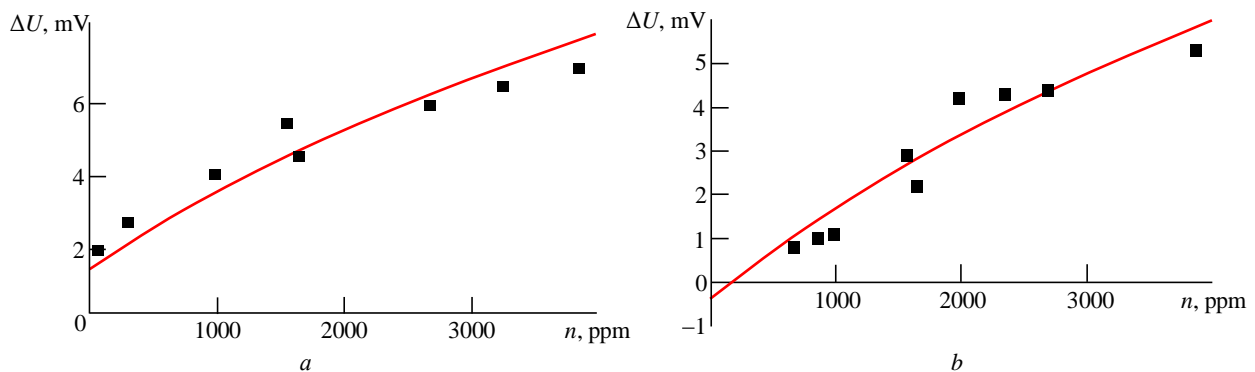

Fig. 3. Ethanol concentration dependence of the potential difference for ZnO/ZnO:Cu structures, produced by dip-coatings into having 3 at. % Cu in the case of upper layer produced by: *a* – two dip-coating cycles; *b* – three dip-coating cycles
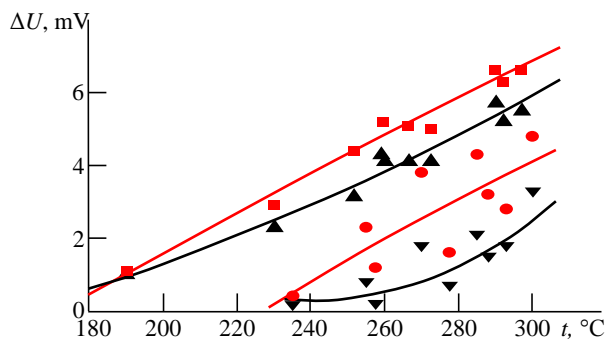
From Gas Sensors to Detection of Etanol Vapour to Sensor of Bacteria Detection

Fig. 4. Temperature dependence of the potential difference for ZnO/ZnO:CuO in the air (▼, ▲) and under exposure of ethanol vapor concentration (●, ■), produced by 4 и 6 immersions in the solution of $Cu(NO_3)_2$

nol vapour with concentration of 1000 ppm. Sensor structures with various CuO contents were studied at various detection temperatures and ethanol vapor concentrations using a device, shown on Fig. 1.

The temperature dependence of the potential difference of nanowire samples ZnO/ZnO:CuO in air and in ethanol vapors at a concentration of 1000 ppm is shown in Fig. 4 [7].

As is seen from Fig. 4, the potential difference between the nanowires of pure and CuO-modified zinc oxide increases with the number of immersions for the nanowire layers formed at 4 and 6 immersions in the $Cu(NO_3)_2$ solution. This phenomenon is caused by the fact that, as the number of immersions increases, a large quantity of ZnO dissolves and then crystallizes in the form of flower-like island structures. The conditions of crystallization of these structures are far from equilibrium; therefore, they contain many defects, including oxygen vacancies and Zn interstitial atoms. As a result, the modulus of thermoelectric coefficient α_{top} (which has a negative value) of the CuO-doped ZnO nanowire layers in the structures under study increases, which favors an increase in the total potential difference (positive value). In the case of the structure formed upon four immersions, the potential difference in air changes nonlinearly, whereas the potential difference in the case of six immersions changes linearly with temperature.

The linear behavior is explained by the fact that ZnO is an *n*-type semiconductor, and its resistance decreases with increasing temperature because of the generation of additional electron–hole pairs. As a result of the generation of electron–hole pairs, thermoelectric coefficient α_{top} of the modified layer in the structure under study becomes high in modulus

(it is a negative value), which leads to an increase in the total potential difference as a positive quantity (see Fig. 4).

The nonlinear character of the temperature dependence of the potential difference in the case of four immersions in the sol is caused by the fact that the crystal structure of the ZnO nanowire layer has a small number of point defects because of a small amount of recrystallized ZnO. When the number of defects is small, the concentration of electrons, which are the main charge carriers in ZnO, is also rather low. In this case, the thickness of a depleted charge region is larger as compared to the structure formed upon six immersions. This feature causes a stronger modulation of thermoelectric coefficient α_{top} of the modified layer because of oxygen ion sorption, which increases the resistance of ZnO [16]. Because of oxygen ion sorption, thermoelectric coefficient α_{top} of the modified layer becomes lower in modulus (it is still negative), which causes a decrease in the potential difference as a positive quantity and leads to a nonlinear increase in the potential difference with temperature of the sample formed upon four immersions.

In both cases, however, the potential difference increases in ethanol vapors, since the electrons trapped during oxygen ion sorption on the surface return to the conduction band of ZnO during the interaction of ion sorbed oxygen with ethanol molecules and, hence, increase the electron concentration in the upper layer. In this case, thermoelectric coefficient α_{top} of the modified layer in the structure under study becomes a more negative quantity and, hence, increases the potential difference as a positive quantity.

It is seen from the temperature dependence of the measured potential difference that the response of the ZnO/ZnO:CuO nanostructures formed upon four immersions under the action of ethanol vapors is significantly higher than in the case of six immersions in the $Cu(NO_3)_2$ solution. This result can be related to the CuO content in the samples. Being a *p*-type semiconductor, CuO adsorbs the molecules having unpaired electrons, such as ethanol and molecular oxygen, and interacts with their unshared electron pairs [17]. After such molecules are adsorbed by the ZnO surface (where ion-sorbed oxygen is inevitably present), the reaction that increases the sensitivity of the structure formed upon four immersions in the solution takes place. As the number of

From Gas Sensors to Detection of Etanol Vapour to Sensor of Bacteria Detection

immersions increases, the quantity of dissolved and recrystallized ZnO increases along with increasing localization of active molecules on the ZnO surface. As a result, the sensitivity of the structure decreases, since the increase in the number of electrons in ZnO that is induced by an increase in the fraction of ZnO containing a large number of point defects leads to a decrease in the Debye length and, hence, to a smaller modulation of the measured potential difference.

4. *Ethanol vapour concentration dependence of* ZnO/ZnO:CuO *junction structures.* The potential difference of the structures under study as a function of the ethanol vapour concentration is also of interest. This dependence is related to the change in the charge transfer caused by the interaction of various numbers of ethanol molecules with the surface of the modified layer in the structures. Some results are presented in Fig. 5 [7], where the ethanol vapor concentration is varied from 0 to 3500 ppm at a working temperature $t = 268 \pm 2$ °C.

It is seen that the sensitivity of the structure of ZnO/ZnO:CuO nanowires formed upon four immersions in the $Cu(NO_3)_2$ solution is higher than that of the structure of ZnO/ZnO:CuO nanowires formed upon six immersions in the $Cu(NO_3)_2$ solution according to the causes described above. However irrespective of the technological conditions of structure formation, the sensitivities of the prepared sensor structures have a nonlinear dependence on the ethanol vapor concentration, which is promising for designing high-sensitivity sensors operating at low temperatures.

Obviously, the potential difference increases noticeably as the ethanol vapor concentration in an air flow increases, which provides the sensitivity of the grown ZnO films to organic molecules. The response of this sensor to ethanol is potentiometric and characterized by a nonlinear dependence of the potential difference on the concentration, according to the
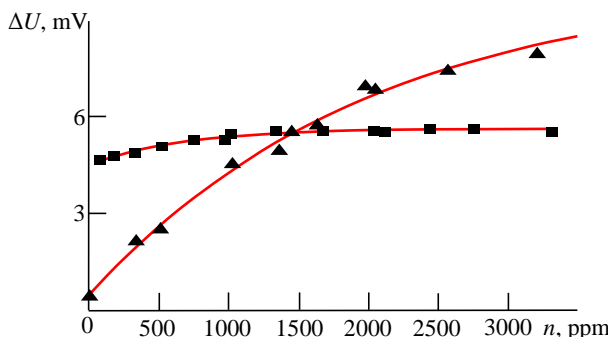
Nernst equation [18]. A change in the CuO concentration in the modified layer also substantially affects the functional properties of the formed structures.

5. *Temperature dependence of the potential difference ofobtained ZnO/ZnO:Fe junctions in air flow and in the flow of mixture of air with ethanol vapour with concentration of 1000 ppm.* Temperature dependence of the of thermo-electromotive force (EMF) (the potential difference) in the air and under 1000 ppm ethanol vapour exposure for ZnO/ZnO:Fe structures having different thickness and morphology of the ZnO:Fe layer is investigated in order to find out the lowest operation temperature with maximum sensitivity (shown in Fig. 6 [8]).

From Fig. 6 it can be seen that the temperature dependence of EMF at the atmosphere for the structure ZnO/ZnO:Fe, produced by two dip-coatings of the upper layer in Fe modified sol have the value of $\Delta U = -8.5$ mV at the temperature of 190 °C. With increasing the temperature, the potential difference is also increasing, passing through $\Delta U = 0$ at the temperature of 240 °C and reaching the value of $\Delta U = 9.5$ mV at the temperature of $t = 295$ °C (Fig. 6). When the upper layer of ZnO/ZnO:Fe structure is produced by three dip-coatings in the Fe modified sol, $\Delta U = 0$ at the temperature of $t = 190$ °C. With increasing the temperature, potential difference increasing almost linearly, reaching the value of $\Delta U = 13.25$ mV at temperature of 350 °C (Fig. 6). It is interesting to note that no mater of number of dip-coatings of the upper layer of the structures, the potential difference of both structures becomes equal to the value $\Delta U = 3.5$ mV at the temperature of $t = 255$ °C. After that the temperature dependence of the potential difference goes almost linearly and very close for both structures.

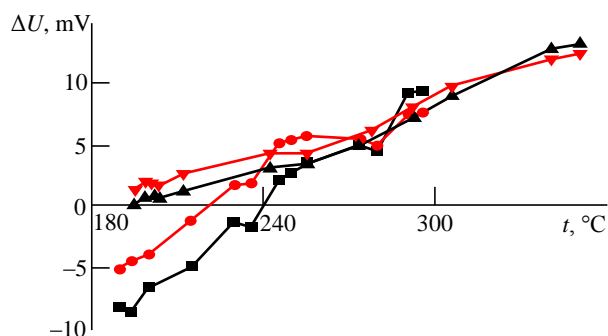Under exposure of ethanol vapours within the the potential difference always increase with the increas-

Fig. 5. Ethanol concentration dependence for the structure ZnO/ZnO:CuO (▲) 4 immersions in solution of $Cu(NO_3)_2$; (■) 6 immersions in solution of $Cu(NO_3)_2$ at detection temperature of 268 ± 2 °C

Fig. 6. Temperature dependence of the potential difference for ZnO/ZnO:Fe structures with upper layer produced by dip - coating into 3 at. % Fe contained sol by means of: ■, ● – two dip-coatings in the sol; ▲ , ▼ – three dip-coatings in the sol, in the air (■,▲) and under 1000 ppm ethanol vapour exposure (●,▼), respectively
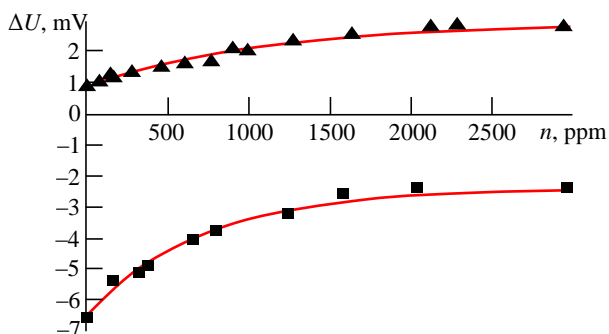
Fig. 7. Ethanol concentration dependence at $t = 200\ °C$ for the ZnO/ZnO:Fe structures with upper layer produced by dip-coating in the sol, containing 3 ат. % for the case of : ■ – two dip-coatings in the sol ; ▲ – three dip-coatings in the sol

ing of the temperature (Fig. 6). The reason for this is the charge transfer because of the interaction between oxygen of ethanol and zinc cation from interstitial site into the Fe–ZnO thin film. We have measured the potential difference of the ZnO/ZnO:Fe structures at operation temperature of 200 °C as function of ethanol vapour concentration. The results are shown in Fig. 7 [8].

As could be seen for the for the ZnO/ZnO:Fe structure with upper layer produced by two dip-coatings in the sol, the measured by us potential difference has negative value over the all of the investigated range of ethanol vapour concentrations and changing from −6.6 mV in the air up to −2.4 mV at the concentration of ethanol vapour 3000 ppm

(Fig. 7). When the upper layer of the ZnO/ZnO:Fe structure is produced by three dip-coatings in the sol, the measured by us potential difference has positive value over the all of the investigated temperature range and changing from 0.9 mV in the air up to 2.8 mV at the concentration of ethanol vapour 3000 ppm (Fig. 7). However, the measured by us potential difference is reaching the saturation value at about 2000 ppm in of the both cases.

Response of ZnO/ZnO:Fe structure to bacterial suspension. 1. *Experimental installation for bacteria detection. Pseudomonas putida* is used as a surrogate of the pathogen *Pseudomonas aeruginosa*, which often causes nosocomial infections. In the present paper we try to produce a biosensor for detection of pathogenic bacteria transmitted by air. That is why we did not test *E.coli*, which is an inhabitant of polluted water.

In order to investigate the sensing properties towards bacteria we have constructed the experimental installation, shown in Fig. 8. All of the blocks used to construct this apparatus are situated at atmospheric pressure into the same thermostatic chamber from polymethylmetacrylate, shown in Fig. 8 [11].

The electronic devices are situated out from this box. This constructive solution has he following advantages: one electronic thermoregulator is used to regulate automatically the temperature of all the blocks included inside the box, not only of
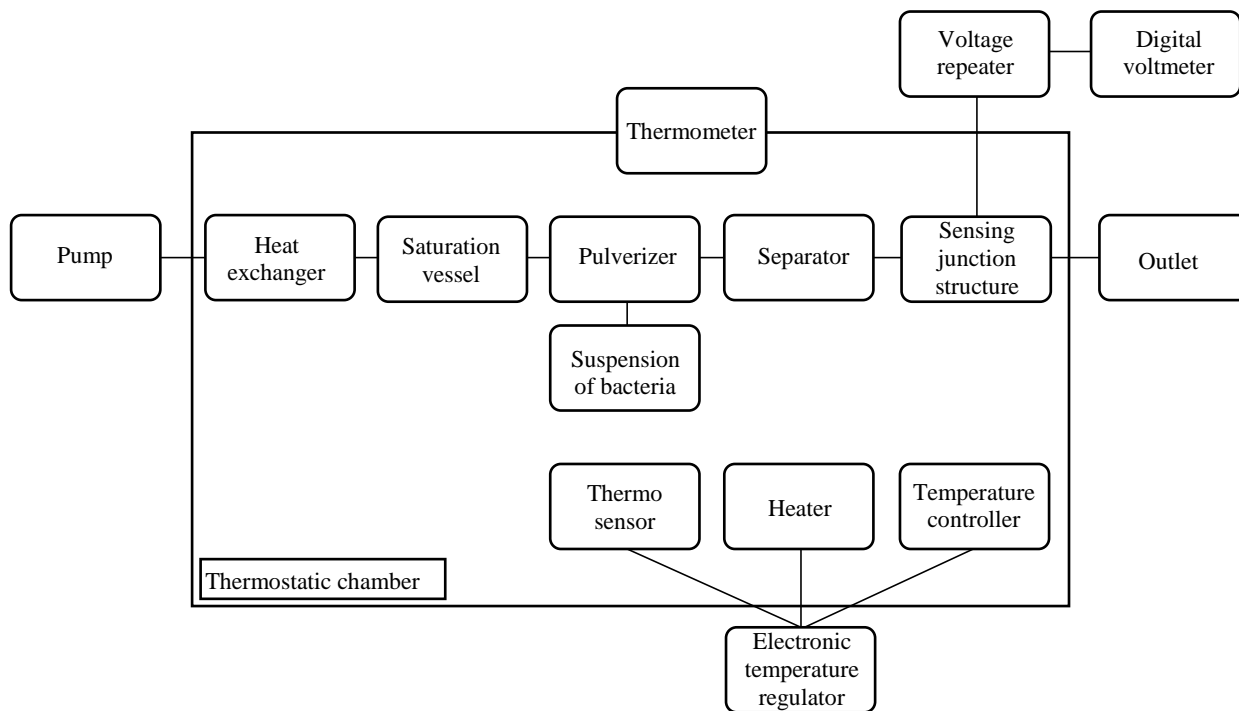

Fig. 8. Experimental installation for bacterial detection

investigated sensing device. By this way there is no reason other devices to be kept at constant temperature and the accuracy of maintaining the temperature of the sensor system is increased.

As it is mention above, the thermostat is constructed from polymethyl metacrylate. The thermostatic chamber is formed from plates with the thickness of about 10 mm. By this way the area of the box is better thermo-isolated from surrounding environment than if the box was constructed by other thermo-isolated materials. In addition of that polymethylmetacrylate allows to control all of occurred processes and it is much stronger in comparison with glass and other transparent materials.

The main part of the apparatus is built on modular principle, which makes its service and repair easy and convenience in modification if nessasary. The functional blocks (modules) following the line of carrier-gas are shown in Fig. 8:

1) the heat exchanger for incoming gas coming from the pump is made in form of copper spiral in order to increase the exchange of heat between the heater and environment by equalization of the temperature of incoming gas flow and stated at the thermostat;

2) the glass G20 saturation vessel is Drexel bottle, having a NS35 polishing on the neck and porosity G1 of the glass bubbler. The purpose of this facility is preliminarily saturation of the carrier gas with water vapour for preventing the bacteria in the aerosol from drying. It can also be used for introducing some substance into the carrier gas;

3) the pulverizer is made from non-corrosive materials, such as stainless steel 314, Polytetrafluoroethylene (Teflon, PTFE) and glass in order to avoid its interaction with working fluids. It is used for dispersion of bacterial suspension into aerosol condition;

4) the separator is made of G20 glass/Pyrex. It is used for removal of large droplets from the aerosol. The aerosol becomes more dispersive and with higher degree of refinement after passing through the separator;

5) well dispersed aerosol interacts with the sensing junction structure and the alterations are monitored by the electronic device. The system for the electrical measurement of experimental set-up includes a digital voltmeter. It has six decimal positions on the screen of display with voltage ranges of 0.1 V with accuracy of 1 μV up to $1 \cdot 10^3 \text{V}$ with accuracy of 1 mV. The coverage of internal resistance

is $R_i \geq 2 \cdot 10^{10} \Omega$ at the ranges of 1 V & 10 V, and $R_i \geq 2 \cdot 10^9 \Omega$ at range of 0.1 V, both of it at direct current. This device has the port for connection with computer and possible distance control. The total description of protocol is reviewed at detailed technical documentation of the device. To increase the input resistance, the complete set of the device included voltage repeater, allowing increasing of R_i up to 10^{13}. The repeater is constructed on the basis of the integral schemes and can be considered as independent unit having an own power supply.

The principle of operation of the electronic temperature regulator shown on Fig. 8, is shown more detailed in Fig. 9 [11].

From there can be seen it consists of Thermo sensor, Heater and Temperature controller. The circulation of air into the thermostat is promoted by small noiseless ventilator, shown on Fig. 9 and covered with a protective cowling. A heater and a circuit-breaker against accidental overheating are also placed into the thermostat. The electronic temperature controller consists of a semiconductor resistance type thermo sensor. It has a cover from stainless steel and copper tip for a good thermal contact with the surrounding environment. The sensor cover is hermetic in order to protect it from accidental effect of harsh exposures.

Regulating the temperature is conducted by heat exchanger, operating on analogous comparison of incoming order and suitably multiplied signal from the temperature sensor. The comparator is a standard integral circuit brand μ723 in corresponding special scheme connection. The order is formed by means of multiturn (helical) potentiometer; the amplification device is combination of part of integral circuit brand part μ723, combined with relay output. The heating element has a power of 300 W. It possesses very low own weight and insignificant heat capacity as well.
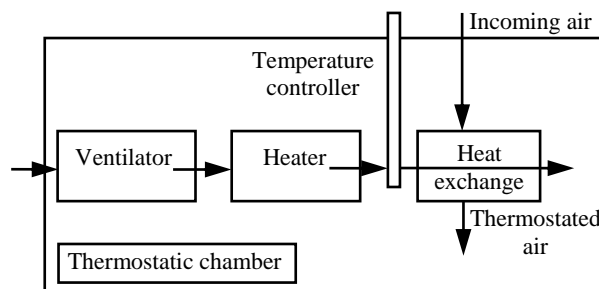

Fig. 9. The temperature regulation into the thermostatic chamber

The last property is necessary for increasing stability of temperature regulation against oscillation after achieving the steady regime.

The holder of the sensing structure is made of materials with high resistance to the working fluids (Fig. 10, *1* – BNC (Bayonet Neill-Concelman) connector; *2* – Bacterial aerosol; *3* – Sensing junction structure; *4* – Beryllium brass springs; *5* – PTFE table; *6* – Holder stage [8]): stainless steel 314, PTFE, silicon rubber, oxigenized aluminium, brass, Pyrex glass. The electrical connection of sensing structure is realized by BNC cable *1*. The sprayed aerosol *2* is deposited directly on the sensing structure *3*. To avoid formation of continuous liquid layer on the sample surface, the flow of the extra liquid down from the sample is ensured. The electric contacts to the sensing structure are in the form of needles. They are made of gilded phosphoric bronze (beryllium bronze). Their pressing with suitable force on the sample surface is realized by two Beryllium Brass springs *4*. The force with which they are pressed on the sample must be strong enough to deform locally the crystal structure of ZnO. This is necessary in order to make different point defects, which perform the Ohmic electrical contacts to ZnO layer. But the force must be not too strong to make the pin holes and to lose electrical connection with the sensing structure. The construction and materials are chosen with high insulation resistance in order to minimize the leakage currents outside from the sensing structure.

The discharge system is designed in order to bring the aerosol out from working area for conceivable disposal. The materials used in construction of this part of the installation are silicone rubber and Pyrex glass. From preventing the outside flow into the experimental system at the output the gas mixture goes out through Drexel bottle filled with Glycerin.

All the building blocks of the experimental set up, which are exposed to the aerosol, can withstand potentially harmful materials and are also resistant to heat sterilization. Because of these considerations as well as taking into account that the system should be transported without difficulties, all of the details which could be exposed to dangerous species are built up as detachable units into a small box made from polymethylmetacrylate.

2. *Microorganisms.* Microorganisms and Cell Cultures (NBIMCC) and is referred as ATCC 12633. It was cultivated in two types of nutrient media: the rich natural one and the poor synthetic medium ISO 12072. The bacterial culture for experiments with the biosensor was prepared from frozen at –15 °C for 24 h. *Pseudomonas putida* culture stored in Eppendorf tubes with glycerol, having density of 10^6 CFU cm^{-3} (CFU – colony-forming unit). The fresh culture was obtained after 24 h cultivation on rich liquid ISO10712 medium at 23…25 °C and three sub-cultivation procedures in liquid pretest medium described also in the same standard ISO10712. After the third sub-cultivation the cells were washed three times with deionized water to remove all ions from the culture medium. As the *Pseudomonas putida* is usual both air and water inhabitant, it could grow and multiply in drinking water. In deionized water the cells could survive up to a month. That is the reason that makes necessary the determination of the live bacterial quantity by means of cultivation methods every time in the day of experiment with the biosensor.

The bacterial suspension in an exponential growth phase (12…18 h) was centrifuged after the third subcultivation in poor synthetic medium at 10 000 rpm for 20 min, the water was decanted and the bacterial pellet was suspended in deionized water. The same wash was repeated 3 times in order to remove all ions from the bacterial cells. The bacterial pellet was kept at 4 °C in 100 μL deionized water. Then at the day of the experiment immediately tenfold dilution was prepared in deionized water, inoculated and cultivated on the rich medium to determine the quantity of survived bacteria. Several dilutions of bacteria were used for the measurements
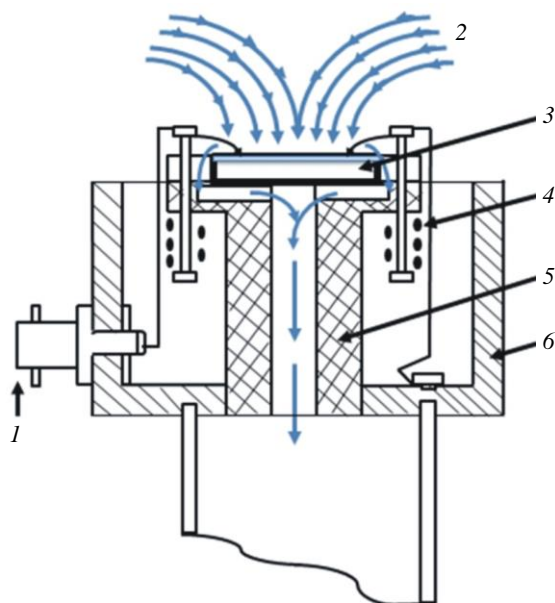

Fig. 10. Holder of the sensing junction structure

From Gas Sensors to Detection of Etanol Vapour to Sensor of Bacteria Detection

of ZnO/ZnO:Fe thin films sensitivity as a function of bacteria amount.

3. *Experimental investigation for bacteria detection as a function of bacteria amount.* For investigating sensing properties of ZnO/ZnO:Fe junction structures to bacteria the thermoelectric potential difference is measured at constant temperature (37 °C) under exposure to air, pulverized water, and pulverized *Pseudomonas putida* suspension. The temperature of the experiment was chosen as intermediate between the most suitable temperature for bacteria to survive and the existing of big enough for detecting potential difference at our sensing structure. The aseptic standards are maintained as all operations are performed in the laminar Bio-hood, which provides a sterile atmosphere. The quantity of live bacteria was determined on nutrient agar medium and every time the purity of the culture was checked by microscope before the experiment with the biosensor. The electrical measurement is performed at least one hour after turning the equipment on. This time was enough for warming up the equipment and stabilization of voltage values on the screen of the potential difference measuring device and the temperature in the box as well. It is established that the response of ZnO/ZnO:Fe junction structures to water vapor is insignificant in comparison to the bacteria's response. In addition of that the amplitude and half-width of the peaks are much smaller in comparison with those under bacterial suspension exposure. It should also be mentioned that both the response and the recovery time in the case of bacterial detection are much slower than in the case of water vapor exposure. Some of the most representative results of alteration of the potential difference under exposure of different amount of *Pseudomonas putida* suspension are shown in Fig. 11. The response of different ZnO/ZnO:Fe junction structures having upper (working) layer produced by: three dip-coating cycles into Fe modified sol (upper part); two dip-coating cycles into Fe modified sol (lower part); under exposure of bacterial suspension of *Pseudomonas putida* (the amount of bacteria is 60, 150, 157 CFU for volume bacterial suspension of 10, 500, 1000 μL, respectively [12]).

The results show that alteration of the potential difference of ZnO/ZnO:Fe junction structures under *Pseudomonas putida* suspension exposure depends strongly on the amount of bacteria suspension. The sensor response of the sensing structures depends on
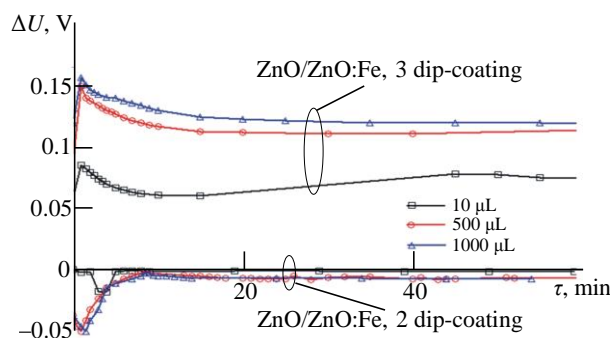

Fig. 11. The response of different ZnO/ZnO:Fe junction structures having upper (working) layer

the surface morphology of the ZnO:Fe films used as working layers of the ZnO/ZnO:Fe junctions. The morphology changes drastically as a function of a number of dip-coating of substrate in the Fe containing sol, as shown in the case, where the response of only geometrically different structures to ethanol vapors is investigated [12]. It is clear that in our case we are not dealing with the interface phenomena,because the changing the number of dip-coatings does not changethe conditions of the interface between the pure and Fe modified ZnO, but changing only structure and morphology, which changing the concentration of charge carriers, affecting by this way the thermoelectric properties of the layers. That is the reason why with changing the number of dip-coating for producingthe upper layer of investigated structures we are able to change even sign of the value of the potential difference. In case of ZnO layer doped with Fe, deposited by two dip-coatings on pure ZnO, the ganglia-like-hills are uniformly situated. Moreover, when ZnO doped with Fe is deposited by three dip-coatings, the average thickness of the ganglia-like-hills is in much larger range in comparison with layer of ZnO doped with Fe produced by two dip-coating in Fe containing sol. Such functional nanostructures with dimensions comparable to Debye's length (~0.3 μm for undoped ZnO at room temperature [19]) are some of the advantages of sol-gel technology, in additional to smoothness, continuity, and a homogeneity of the composition [8]. As expected, the response to bacterial suspension is completely different in the cases of different surface morphology. For the ZnO/ZnO:Fe junction structure which has upper (working) Fe modified ZnO layer produced by three dip- coating cycles into the Fe modified sol, the potential difference has a positive value and increases with increasing the amount of the pulverized bacteria (upper part in Fig. 11). When

dealing with ZnO/ZnO:Fe junction structure which has upper (working) Fe modified ZnO layer produced by two dip-coating cycles into the Fe modified sol, the situation is completely different. In the second case, the potential difference has a negative value and decreases with increasing the amount of the pulverized bacteria (down part in Fig. 11).

Summary of main results from this work. The main results of this work could be summarized as follows:

1) we have found that for the ZnO/ZnO:Cu junction structures ability to detect ethanol vapour, the top layer must be formed of three dip-coatings into the sol, containing 3 at.% Cu and the lower layer must be pure ZnO. In this case the maximum of sensitivity to ethanol vapour is at temperature of 278 °C;

2) the response of ZnO/ZnO:CuO nanowires junction structures formed upon four immersions under the action of ethanol vapors is significantly higher than in the case of six immersions in the $Cu(NO_3)_2$ solution. In this case the maximum of sensitivity to ethanol vapour is at temperature of 268 °C;

3) the sensitivity to bacterial suspension of ZnO/ZnO:Fe sensing structures, with upper (working) layer produced by two dip-coating cycles, is much higher than the sensitivity of ZnO/ZnO:Fe structures, with upper (working) layer produced by three dip-coatings. When dealing with ZnO/ZnO:Fe junction structure which upper (working) Fe modi-

fied ZnO layer is produced by two dip-coating cycles into the Fe modified sol, the potential difference has a negative value and decreases with increasing the amount of the pulverized bacteria.

Conclusions. Based on measurements done on different sensing junction structures, investigate in this work, we discovered that ZnO/ZnO:Fe structure, with upper layer, produced by two dip-coating in th sol, has the lowest operation temperature of 200 °C. This operation temperature is a bit higher than operation temperature of 300 K presented in [9] and 100 °C [13] at which some very novel sensing structures show the maximum sensitivity. The measured by us potential difference has negative value over the all of the investigated range of ethanol vapour concentrations and changing from −6.6 mV in the air up to −2.4 mV at the concentration of ethanol vapour 3000 ppm. For the ZnO/ZnO:Fe junction structure which has upper (working) Fe modified ZnO layer produced by three dip- coating cycles into the Fe modified sol, the potential difference has a positive value and increases with increasing the amount of the pulverized bacteria. When dealing with ZnO/ZnO:Fe junction structure which has upper (working) Fe modified ZnO layer produced by two dip-coating cycles into the Fe modified sol, the potential difference has a negative value and decreases with increasing the amount of the pulverized bacteria

References

1. Wolkenstein F. F. Electronic Processes at the Surface of SemiconductorsDuring the Chemosorptions. 1st ed. Moscow, *Nauka*, 1987, 432 p. (In Russ.)

2. Xu J., Han J., Zhang Y., Sun Y., Xie B. Studies on Alcohol Sensing Mechanism of ZnO Based Gas Sensors. Sens. Actuators B. 2008, vol. 132(1), pp. 334–339. doi: 10.1016/j.snb.2008.01.062

3. Comini E. Metal Oxide Nano-Crystals for Gas Sensing. Anal. Chim. Acta. 2006, vol. 568 (1–2), pp. 28–40. doi: 10.1016/j.aca.2005.10.069

4. Paraguay D. F., Miki-Yoshida M., Morales J., Solis J., Estrada L.W. Influence of Al, In Cu, Fe and Sn Dopants on the Response of Thin Film ZnO Gas Sensor to Ethanol Vapour. Thin Solid Films. 2000, vol. 373, pp. 137–140. doi: 10.1016/S0040-6090(00)01120-2

5. Stambolova I., Konstantinov K., Vassilev S., Peshev P., Tsacheva T. Lanthanumdoped SnO_2 and ZnO Thin Films Sensitive to Ethanol and Humidity. Mater.Chem. Phys. 2000, vol. 63 (2), pp. 104–108. doi: 10.1016/S0254-0584(99)00193-5

6. Dimitrov D. Tz., Nikolaev N. K., Papazova K. I., Krasteva L. K., Pronin I. A., Averin I. A., Bojinova A. S.,

Georgieva A. Ts., Yakushova N. D., Peshkova T. V., Karmanov A. A., Kaneva N. V., Moshnikov V. A. Investigation of the Electrical and Ethanol-Vapour Sensing Properties of the Junctions Based on ZnO Nanostructured Thin Film Doped with Copper. Appl. Surf. Sci. 2017, vol. 392, pp. 95–108. doi: 10.1016/j.apsusc.2016.08.049

7. Peshkova T. V., Dimitrov D. Ts., Nalimova S. S., Kononova I. E., Nikolaev N. K., Papazova K. I., Bozhinova A. S., Moshnikov V. A., Terukov E. I. Structures of Nanowires with ZnO–ZnO:CuO Junctions for Detecting Ethanol Vapors. Tech. Phys. 2014, vol. 59 (5), pp. 771–776. doi: 10.1134/S1063784214050259

8. Pronin I. A., Dimitrov D. Tz., Krasteva L. K., Papazova K. I., Averin I. A., Chanachev A. S., Bojinova A. S., Georgieva A. Ts., Yakushova N. D., Moshnikov V. A. Theoretical and Experimental Investigations of Ethanol Vapour Sensitive Properties of Junctions Composed from Produced by Sol-Gel Technology Pure and Fe Modified Nanostructured ZnO Thin Films. Sens. Actuators A. 2014, vol. 206, pp. 88–96. doi: 10.1016/j.sna.2013.11.035

9. Kuo G.-H., Wang H. P., Hsu H. H., Wang J., Chiu Y. M., Jou C.-J. G, Hsu T. F., Chen F.-L. Sensing of Ethanol with

Nanosize Fe–ZnO Thin Films. J. Nanomater. 2009, vol. 2009, Article ID 316035. doi: 10.1155/2009/316035

10. Nirmala M., Anukalian A. Synthesis and Characterization of Undoped and TM (Co, Mn) Doped ZnO Nanoparticles. Mater. Lett. 2011, vol. 65 (17–18), pp. 2645–2648. doi: 10.1016/j.matlet.2011.06.029

11. Dimitrov D. Tz., Krasteva L. K., Lyutov L. G., Pronin I. A., Ivanova I. A., Kaneva N. V., Papazova K. I., Averin I. A., Bojinova A. S., Yakushova N. D., Georgieva A. Ts., Moshnikov V. A. Experimental Investigation and Modeling of Bio-Sensitive Properties of ZnO/ZnO:Fe Junctions Based on Nanostructured Films Produced by Sol-Gel Technology. Pt. I. Mater. Sci. Technol. 2016, vol. 24 (2), pp. 77–91.

12. Dimitrov D. Tz., Krasteva L. K., Lyutov L. G., Pronin I. A., Ivanova I. A., Kaneva N. V., Papazova K. I., Averin I. A., Bojinova A. S., Yakushova N. D., Georgieva A. Ts., Moshnikov V. A. Experimental Investigation and Modeling of Bio-Sensitive Properties of ZnO/ZnO:Fe Junctions Based on Nanostructured Films Produced by Sol-Gel Technology. Pt. II. Mater. Sci. Technol. 2016, vol. 24 (3), pp. 127–142.

13. Hsueh T.-J, Hsu C.-L. Fabrication of Gas Sensing Devices with ZnO Nanostructure by the Low-Temperature Oxidation of Zinc Particles. Sens. Actuators B. 2008, vol. 131 (2), pp. 572–576. doi: 10.1016/j.snb.2007.12.045

14. Stilbans L. S. *Fizika poluprovodnikov* [Semiconductor Physics]. 1st ed. Moscow, *Sovetskoe radio*, 1967, 451 p. (In Russ.)

15. Kaneva N., Stefanov B., Dimitrov D., Dushkin C. Photocatalytic Degradation of Methylene Blue by ZnO Photocatalyst Doped with Nickel. Ann. Univ. Sofia (Fac. Chim.) 2011, vol. 102/103, pp. 293–304.

16. Takata M., Tsubone D., Yanagida H. Dependence of Electrical Conductivity of ZnO on Degree of Sintering. J. Am. Ceram. Soc. 1976, vol. 59 (1–2), pp. 4–8. doi: 10.1111/j.1151-2916.1976.tb09374.x

17. Gopel W. Solid-State Chemical Sensors: Atomistic Models and Research Trends. 1989, vol. 16 (1–2), pp. 167–193. doi: 10.1016/0250-6874(89)80015-0

18. Dimitrov D. Tz., Anastasova S. Y., Dushkin C. D. Oxygen Sensing Junctions Based on Yttria Stabilized Zirconia with Platinum Nanoparticles. Rev. Sci. Instrum. 2006, vol. 77, pp. 0561081–0561083. doi: 10.1063/1.2202925

19. Ri S., Hamano K., Nakagawa Z. Debye Length and Gas Sensor Mechanism of Undoped and Sm_2O_3-Doped ZnO Ceramics. Ceram. Soc. Jpn. 1986, vol. 94, pp. 419–424. doi: 10.2109/jcersj1950.94.1088_419

Information about the author

Dimitre Tz. Dimitrov, PhD (Eng.) (1998), Associate Professor of the Department of Inorganic Chemistry at the Sofia University St. Kliment Ohridski, Bulgaria and head of the Laboratory of Nanoparticle Science and Technology there. He is the author of 53 scientific publications. Area of expertise: photocatalysis; sensors and biosensors.
Address: Sofia University St. Kliment Ohridski, 15 Tsar Osvoboditel Blvd., Sofia 1504, Bulgaria
E-mail: nhddt@chem.uni-sofia.bg; dimitrov2001@yahoo.com
https://orcid.org/0000-0001-5451-1189